Biochemistry

pubs.acs.org/biochemistry

Communication

# Enhanced Cholesterol-Dependent Hemifusion by Internal Fusion Peptide 1 of SARS Coronavirus-2 Compared to Its N-Terminal Counterpart

Gourab Prasad Pattnaik, Surajit Bhattacharjya,* and Hirak Chakraborty*

Cite This: *Biochemistry* 2021, 60, 559−562

Read Online

ACCESS | Metrics & More | Article Recommendations | Supporting Information

**ABSTRACT:** Membrane fusion is an important step for the entry of the lipid-sheathed viruses into the host cells. The fusion process is being carried out by fusion proteins present in the viral envelope. The class I virus contains a 20−25 amino acid sequence at its N-terminal of the fusion domain, which is instrumental in fusion and is called as a "fusion peptide". However, severe acute respiratory syndrome (SARS) coronaviruses contain more than one fusion peptide sequences. We have shown that the internal fusion peptide 1 (IFP1) of SARS-CoV-2 is far more efficient than its N-terminal counterpart (FP) to induce hemifusion between small unilamellar vesicles. Moreover, the ability of IFP1 to induce hemifusion formation increases dramatically with growing cholesterol content in the membrane. Interestingly, IFP1 is capable of inducing hemifusion but fails to open the pore.

Membrane fusion is a crucial step for successful entry and infection of the enveloped viruses, leading to the transfer of viral genetic materials into the host cell.[1−5] The fusion event is triggered by the viral fusion protein that comes into action after the receptor-binding domain interacts with the cell surface receptor proteins.[6] Generally, for class I viruses, a 20−25 amino acid stretch present in the N-terminus of the fusion protein is known as a fusion peptide, which is instrumental in binding with the host cell, and initiating the fusion process.[7,8] Severe acute respiratory syndrome (SARS) is an emerging form of pneumonia caused by SARS-CoVs, and the entire world is now going through a crisis due to the attack of SARS-CoV-2. The fusion domain of SARS-CoV spike protein (S2) contains three putative fusion peptides recognized as the N-terminal fusion peptide (FP), internal fusion peptide 1 (IFP1), and internal fusion peptide 2 (IFP2).[9−13] The S2 protein contains heptad repeats, HR1 and HR2, and a transmembrane region at the C-terminus in addition to these fusion peptides. Interestingly, the FP and IFP1 are highly homologous between SARS-CoV-1 and SARS-CoV-2 (Table 1). Therefore, a proper understanding of the role of FP and IFP1 in inducing membrane fusion would provide valuable mechanistic insights into the entry of both SARS-CoV-1 and SARS-CoV-2. The atomic resolution structure of the complex formed by two heptad regions revealed the formation of a six-helix bundle, considered to facilitate close apposition of two fusing membranes.[14,15] Membrane composition plays a significant role in the fusion process as it alters the fusion protein or peptide conformation as well as the membrane organization and dynamics.[16] The role of cholesterol in membrane fusion is firmly established from the results obtained from viral and model membrane fusion.[17,18] Cholesterol is also known to promote oligomerization of the SARS-CoV FP.[19]

**Table 1. Sequences of FP and IFP1 for SARS-CoV-1, SARS-CoV-2, and Peptides Used in the Study**

| | |
|---|---|
| Fusion Peptide | |
| SARS-CoV-1 | MYKTPTLKDFGGFNFSQIL |
| SARS-CoV-2 | IYKTPTLKDFGGFNFSQIL |
| Internal Fusion Peptide 1 | |
| SARS-CoV-1 | GAALQIPFAMQMAYRF |
| SARS-CoV-2 | GAALQIPFAMQMAYRF |

The lipid stalk hypothesis assumes the sequential evolution of the intermediates toward the opening of the fusion pore. Initially, two bilayers come close, and the outer leaflets of both bilayers mix to form the stalk intermediate. Subsequently, the inner leaflets of the apposed membranes come in contact with each other to form transmembrane contact, which finally undergoes mixing of inner leaflets to open the fusion pore. The stalk and transmembrane contact structures are collectively called hemifusion intermediates. A schematic representation of the fusion process is shown in Scheme 1.

In this work, we have studied the effectiveness of FP and IFP1-induced fusion of small unilamellar vesicles (SUVs), and evaluated the effect of membrane cholesterol on the fusion process. Our results demonstrate that the IFP1 promotes lipid mixing in a cholesterol-dependent fashion. Both the rate and extent of lipid mixing increase significantly in the presence of cholesterol. On the contrary, the FP is not that efficient to induce lipid mixing; however, there is a slight increase in the rate and extent of lipid mixing in the presence of membrane

**Received:** January 15, 2021
**Revised:** February 8, 2021
**Published:** February 11, 2021

**Scheme 1. Schematic Representation of Different Intermediates during the Course of Membrane Fusion**

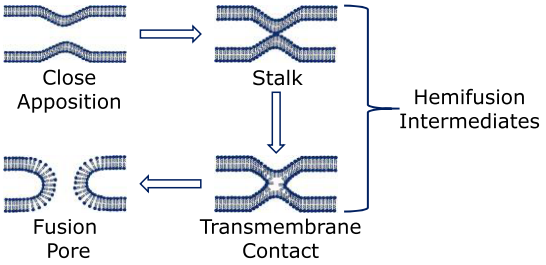


cholesterol. Interestingly, both FP and IFP1 fail to demonstrate substantial content mixing, highlighting the role of other domains of S2 protein for the pore formation. The extent of content leakage remains about 10%, which confirms the overall integrity of fusing membranes.

The above observation indicates that the IFP1 (and partially FP) induces hemifusion but is incapable of opening the pore between two fusing membranes. Our results support the requirement of interaction between FP and transmembrane domain of fusion protein for pore opening as proposed earlier in HIV.[20]

In order to evaluate the effect of FP and IFP1 in membrane fusion, we have measured lipid mixing, content mixing, and content leakage kinetics using fluorescence-based methodologies described in the method section in the Supporting Information. IFP1 induced about 51% of lipid mixing in DOPC/DPOE/DOPG (60/30/10 mol %) SUVs in a lipid-to-peptide ratio of 100:1. The rate and extent of lipid mixing increases with increasing cholesterol concentration, and extents are about 71% and 84% in DOPC/DOPE/DOPG/CH (50/30/10/10 mol %) and DOPC/DOPE/DOPG/CH (40/30/10/20 mol %) SUVs, respectively (Figure 1A, Table 2). This result suggests that the efficiency of IFP1 in promoting lipid mixing is extremely dependent on the concentration of membrane cholesterol, although it promotes a significant amount of lipid mixing, does not induce content mixing, and brings about 10% content leakage in the membrane containing 20 mol % of cholesterol (Figure 1B,C). Putting this observation in the context of membrane fusion, it is clear that the IFP1 is capable of inducing the hemifusion intermediate formation but unable to open the fusion pore. The hemifusion is solely dependent on lipid mixing, where the lipids of outer leaflets of two fusing membranes mix with each other. A small amount of content mixing in the hemifusion intermediate is possible as the small fluorophores can move from one membrane to the other through thermal fluctuation. Moderately low content leakage indicates the overall integrity of the membrane during the formation of hemifusion intermediates. Interestingly, the content leakage data saturates within about 400 s, which designates that the content leakage is majorly observed during the lipid reorganization, forming the hemifusion intermediate. Similar experiments were carried out in three different lipid compositions with the N-terminal FP, and the results are shown in Figure 2A−C. The FP promotes a nominal amount of lipid mixing in all three lipid compositions in a lipid-to-peptide ratio of 100:1. The extent of content mixing and content leakage are similar to what we observed in the presence of IFP1. Overall, our result suggests that the N-terminal FP is less efficient in promoting hemifusion, FP does not rupture the membrane as evident from the moderately low

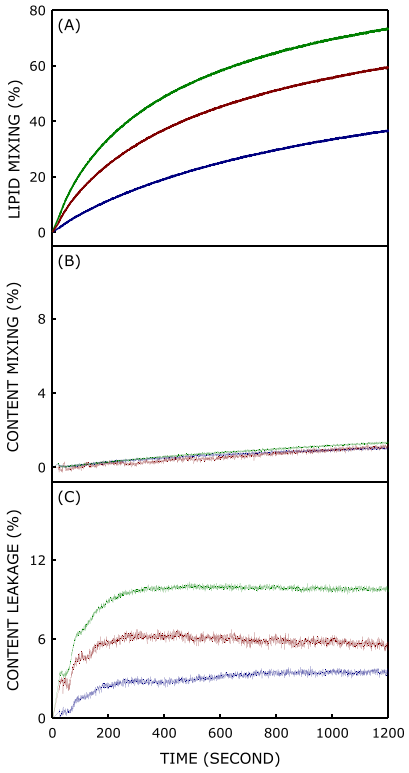


**Figure 1.** Effect of SARS-CoV IFP1 on the kinetics of (A) lipid mixing, (B) content mixing, and (C) content leakage in SUVs containing 0 mol % (blue), 10 mol % (red), and 20 mol % (green) of cholesterol at 37 °C, keeping a lipid-to-peptide ratio of 100:1. See the Supporting Information for more details.

**Table 2. Extent and Rate Constant of Lipid Mixing in the Presence of FP and IFP1 in Different Lipid Compositions**

| Lipid Composition | Peptide | Lipid Mixing (%) | $k$ ($sec^{-1}$) |
|---|---|---|---|
| DOPC/DOPE/DOPG(60/30/10) | IFP1 | 50.8 | $1.3 \times 10^{-3}$ |
| | FP | 3.5 | $8.8 \times 10^{-5}$ |
| DOPC/DOPE/DOPG/CH (50/30/10/10) | IFP1 | 71.4 | $2.0 \times 10^{-3}$ |
| | FP | 8.9 | $6.5 \times 10^{-4}$ |
| DOPC/DOPE/DOPG/CH (40/30/10/20) | IFP1 | 83.6 | $2.3 \times 10^{-3}$ |
| | FP | 11.5 | $8.2 \times 10^{-4}$ |

content leakage, and content leakage majorly takes place during the formation of the hemifusion intermediate.

Generally, for the entry of class I viruses, the N-terminal FP is considered to be crucial. Though SARS-coronaviruses belong to the class I category, our results demonstrated that IFP1 is more fusogenic than its N-terminal counterpart. The higher fusogenicity of IFP1 could be correlated to its higher hydrophobicity compared to the N-terminal FP. The Kyte−Doolittle plot with a running average of seven residues indicates that IFP1 and FP markedly differ in hydrophobicity (Figure 3).[21] Note, 3D structures and localization of FP and IFP1 in membrane mimetic environments are determined by NMR spectroscopy and demonstrated that IFP1 displays a much deeper insertion into the hydrophobic core of the micelle compared to the FP.[22]

Our results further demonstrated the important role of cholesterol in the enhancement of IFP1 and FP-induced hemifusion, an important link between the membrane cholesterol and higher risk of viral infection. The stringency


https://dx.doi.org/10.1021/acs.biochem.1c00046
Biochemistry 2021, 60, 559−562

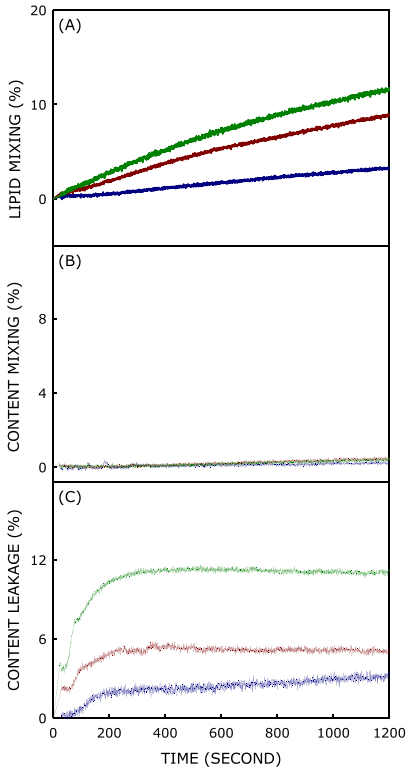


**Figure 2.** Effect of SARS-CoV FP on the kinetics of (A) lipid mixing, (B) content mixing, and (C) content leakage in SUVs containing 0 mol % (blue), 10 mol % (red), and 20 mol % (green) of cholesterol at 37 °C, keeping a lipid-to-peptide ratio of 100:1. See the Supporting Information for more details.

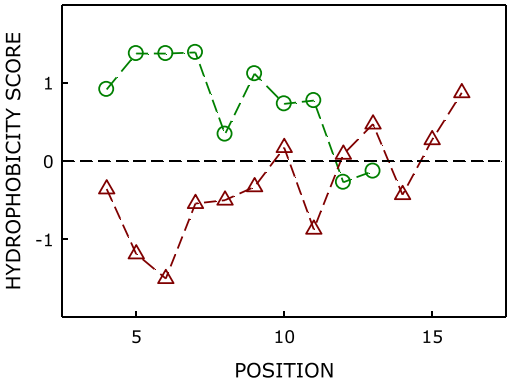


**Figure 3.** Hydrophobicity scores measured with a running average of seven residues of IFP1 (green, circle) and FP (red, triangle) have been plotted against the residue position. Hydrophobicity scores have been taken from the Kyte−Doolittle scale.

of cholesterol in the class I viral infection has been shown earlier, and our results indicate that the higher fusogenicity could be due to the higher effectiveness of fusion peptides in inducing the hemifusion intermediate in the presence of cholesterol. Cholesterol might promote membrane fusion either by modulating the peptide conformation[23,24] and depth of penetration[18] or changing physical membrane properties such as intrinsic negative curvature and stiffness.[25] Cholesterol has an inverted cone-like structure that generates intrinsic negative curvature to the membrane, which promotes the formation of nonlamellar fusion intermediates. In addition, cholesterol enhances overall membrane stiffness, which provides mechanical stability to the highly curved intermediate structures.

In spite of being so successful in inducing hemifusion, both IFP1 and FP fail to open the fusion pore between two fusing membranes. It was shown that the fusion peptide interacts with the transmembrane domain of the fusion protein to open up the pore.[20] The limited ability of the fusion peptides to open up the pore in our study further supports the hypothesis of an interaction between fusion peptide and transmembrane domain to open the fusion pore.

Taken together, our work provides three important pieces of information regarding the fusion peptide-induced membrane fusion for SARS-coronaviruses. First, it is clearly demonstrated that the IFP1 is more fusogenic than the FP, and it could be due to the higher hydrophobicity of IFP1. Second, the importance of cholesterol in the peptide induced membrane fusion and, finally, the requirement of interaction between the fusion peptide and transmembrane domain for pore opening.

## ■ ASSOCIATED CONTENT

### Supporting Information

The Supporting Information is available free of charge at https://pubs.acs.org/doi/10.1021/acs.biochem.1c00046.

Materials and methods (PDF)

## ■ AUTHOR INFORMATION


### Corresponding Authors

**Surajit Bhattacharjya** − *School of Biological Sciences, Nanyang Technological University, 637551, Singapore;* orcid.org/0000-0001-7015-1937; Email: surajit@ntu.edu.sg

**Hirak Chakraborty** − *School of Chemistry and Centre of Excellence in Natural Products and Therapeutics, Sambalpur University, Burla, Odisha 768 019, India;* orcid.org/0000-0001-7499-5707; Email: hirakchakraborty@gmail.com

### Author

**Gourab Prasad Pattnaik** − *School of Chemistry, Sambalpur University, Burla, Odisha 768 019, India*

Complete contact information is available at: https://pubs.acs.org/10.1021/acs.biochem.1c00046


### Author Contributions

G.P.P. performed all of the experiments, analyzed the results, and wrote the initial draft of the manuscript. S.B. and H.C. conceptualized the research, analyzed the results, and wrote the final manuscript.


### Funding

This work was supported by a research grant from the Science and Technology Department, Government of Odisha, awarded to H.C. S.B. acknowledges support from the Ministry of Education (MOE), Singapore.


### Notes

The authors declare no competing financial interest.

## ■ ACKNOWLEDGMENTS


This work was supported by a research grant from the Department of Science and Technology, Government of Odisha, awarded to H.C. S.B. acknowledges support from the Ministry of Education (MOE), Singapore. H.C. and G.P.P thanks the University Grants Commission (UGC) for the

UGC-Assistant Professor position and the Council for Science and Industrial Research, Government of India, for a Senior Research Fellowship, respectively. We acknowledge the Department of Science and Technology, New Delhi, and UGC for providing the instrument facility, School of Chemistry, Sambalpur University, under the FIST and DRS programs, respectively. We thank Dr. S. N. Sahu from the School of Chemistry, Sambalpur University, Dr. S. Haldar from the Gandhi Institute of Technology and Management, and members of the Chakraborty laboratory for their comments and discussions.

## ■ ABBREVIATIONS

FP, fusion peptide; IFP1, internal fusion peptide 1; IFP2, internal fusion peptide 2

## ■ REFERENCES

(1) Skehel, J. J., and Wiley, D. C. (2000) Receptor binding and membrane fusion in virus entry: the influenza hemagglutinin. *Annu. Rev. Biochem. 69*, 531−569.
(2) Hughson, F. M. (1997) Enveloped viruses: a common mode of membrane fusion? *Curr. Biol. 7*, R565−R569.
(3) Freed, E. O., Myers, D. J., and Risser, R. (1990) Characterization of the fusion domain of the human immunodeficiency virus type 1 envelope glycoprotein gp41. *Proc. Natl. Acad. Sci. U. S. A. 87*, 4650−4654.
(4) Dimitrov, D. S., Golding, H., and Blumenthal, R. (1991) Initial stages of HIV-1 envelope glycoprotein-mediated cell fusion monitored by a new assay based on redistribution of fluorescent dyes. *AIDS Res. Hum. Retroviruses 7*, 799−805.
(5) Earp, L. J., Delos, S. E., Park, H. E., and White, J. M. (2004) The many mechanisms of viral membrane fusion proteins. *Curr. Top. Microbiol. Immunol. 285*, 25−66.
(6) White, J. M., Delos, S. E., Brecher, M., and Schornberg, K. (2008) Structures and mechanisms of viral membrane fusion proteins: multiple variations on a common theme. *Crit. Rev. Biochem. Mol. Biol. 43*, 189−219.
(7) Gething, M. J., Doms, R. W., York, D., and White, J. (1986) Studies on the mechanism of membrane fusion: site-specific mutagenesis of the hemagglutinin of influenza virus. *J. Cell Biol. 102*, 11−23.
(8) Durrer, P., Galli, C., Hoenke, S., Corti, C., Glück, R., Vorherr, T., and Brunner, J. (1996) H+-induced membrane insertion of influenza virus hemagglutinin involves the HA2 amino-terminal fusion peptide but not the coiled coil region. *J. Biol. Chem. 271*, 13417−13421.
(9) Madu, I. G., Roth, S. L., Belouzard, S., and Whittaker, G. R. (2009) Characterization of a highly conserved domain within the severe acute respiratory syndrome coronavirus spike protein S2 domain with characteristics of a viral fusion peptide. *J. Virol. 83*, 7411−7421.
(10) Mahajan, M., Chatterjee, D., Bhuvaneswari, K., Pillay, S., and Bhattacharjya, S. (2018) NMR structure and localization of a large fragment of the SARS-CoV fusion protein: Implications in viral cell fusion. *Biochim. Biophys. Acta, Biomembr. 1860*, 407−415.
(11) Sainz, B., Jr., Rausch, J. M., Gallaher, W. R., Garry, R. F., and Wimley, W. C. (2005) Identification and characterization of the putative fusion peptide of the severe acute respiratory syndrome-associated coronavirus spike protein. *J. Virol. 79*, 7195−7206.
(12) Guillén, J., Pérez-Berná, A. J., Moreno, M. R., and Villalaín, J. (2008) A second SARS-CoV S2 glycoprotein internal membrane-active peptide. Biophysical characterization and membrane interaction. *Biochemistry 47*, 8214−8224.
(13) Chakraborty, H., and Bhattacharjya, S. (2020) Mechanistic insights of host cell fusion of SARS-CoV-1 and SARS-CoV-2 from atomic resolution structure and membrane dynamics. *Biophys. Chem. 265*, 106438.
(14) Walls, A. C., Park, Y. J., Tortorici, M. A., Wall, A., McGuire, A. T., and Veesler, D. (2020) Structure, Function, and Antigenicity of the SARS-CoV-2 Spike Glycoprotein. *Cell 181*, 281−292.
(15) DuBois, R. M., Zaraket, H., Reddivari, M., Heath, R. J., White, S. W., and Russell, C. J. (2011) Acid stability of the hemagglutinin protein regulates H5N1 influenza virus pathogenicity. *PLoS Pathog. 7*, No. e1002398.
(16) Meher, G., and Chakraborty, H. (2019) Membrane Composition Modulates Fusion by Altering Membrane Properties and Fusion Peptide Structure. *J. Membr. Biol. 252*, 261−272.
(17) Liu, K. N., and Boxer, S. G. (2020) Target Membrane Cholesterol Modulates Single Influenza Virus Membrane Fusion Efficiency but Not Rate. *Biophys. J. 118*, 2426−2433.
(18) Pattnaik, G. P., and Chakraborty, H. (2019) Cholesterol alters the inhibitory efficiency of peptide-based membrane fusion inhibitor. *Biochim. Biophys. Acta, Biomembr. 1861*, 183056.
(19) Meher, G., Bhattacharjya, S., and Chakraborty, H. (2019) Membrane Cholesterol Modulates Oligomeric Status and Peptide-Membrane Interaction of Severe Acute Respiratory Syndrome Coronavirus Fusion Peptide. *J. Phys. Chem. B 123*, 10654−10662.
(20) Reuven, E. M., Dadon, Y., Viard, M., Manukovsky, N., Blumenthal, R., and Shai, Y. (2012) HIV-1 gp41 transmembrane domain interacts with the fusion peptide: implication in lipid mixing and inhibition of virus-cell fusion. *Biochemistry 51*, 2867−2878.
(21) Kyte, J., and Doolittle, R. F. (1982) A simple method for displaying the hydropathic character of a protein. *J. Mol. Biol. 157*, 105−132.
(22) Mahajan, M., and Bhattacharjya, S. (2015) NMR structures and localization of the potential fusion peptides and the pre-trans-membrane region of SARS-CoV: Implications in membrane fusion. *Biochim. Biophys. Acta, Biomembr. 1848*, 721−730.
(23) Qiang, W., Bodner, M. L., and Weliky, D. P. (2008) Solid-state NMR spectroscopy of human immunodeficiency virus fusion peptides associated with host-cell-like membranes: 2D correlation spectra and distance measurements support a fully extended conformation and models for specific antiparallel strand registries. *J. Am. Chem. Soc. 130*, 5459−5471.
(24) Schmick, S. D., and Weliky, D. P. (2010) Major antiparallel and minor parallel $\beta$ sheet populations detected in the membrane-associated human immunodeficiency virus fusion peptide. *Biochemistry 49*, 10623−10635.
(25) McMahon, H. T., and Boucrot, E. (2015) Membrane curvature at a glance. *J. Cell Sci. 128*, 1065−1070.


https://dx.doi.org/10.1021/acs.biochem.1c00046
*Biochemistry* 2021, 60, 559−562